INSTITUTE OF PHYSICS PUBLISHING EUROPEAN JOURNAL OF PHYSICS

Eur. J. Phys. **28** (2007) 311–320 doi:10.1088/0143-0807/28/2/016

Introductory analysis of Bénard–Marangoni convection

J A Maroto[1], V Pérez-Muñuzuri[2] and M S Romero-Cano[3]

[1] Group of Physics and Chemistry of Linares, Escuela Politécnica Superior, St Alfonso X El Sabio, 28, University of Jaén, E-23700 Linares, Jaén, Spain
[2] Group of Nonlinear Physics, University of Santiago de Compostela, E-15782 Santiago de Compostela, Spain
[3] Group of Complex Fluids Physics, Department of Applied Physics, University of Almería, E-04120 Almería, Spain

E-mail: jamaroto@ujaen.es, vicente.perez@cesga.es and msromero@ual.es

Received 2 October 2006, in final form 26 December 2006
Published 9 February 2007
Online at stacks.iop.org/EJP/28/311

Abstract

We describe experiments on Bénard–Marangoni convection which permit a useful understanding of the main concepts involved in this phenomenon such as, for example, Bénard cells, aspect ratio, Rayleigh and Marangoni numbers, Crispation number and critical conditions. In spite of the complexity of convection theory, we carry out a simple and introductory analysis which has the additional advantage of providing very suggestive experiments. As a consequence, we recommend our device for use as a laboratory experiment for undergraduate students of the thermodynamics of nonlinear and fluid physics.

1. Introduction

Bénard convection, sometimes referred to as Bénard–Marangoni convection (and hereafter abbreviated to BM convection) was first observed by Henri Bénard [1] near the turn of the 20th century. His experimental apparatus was designed to study the behaviour of a thin layer of spermaceti (whale oil) on a metallic plate suspended above a boiling water bath at approximately 100° C. In this experiment, the horizontal extent of the spermaceti surface was much greater than its depth, and Bénard observed the ordered formation of hexagonal cells far away from the boundaries of the container. He determined correctly that warm fluid was flowing up in the centres of the convection cells, and down at the hexagonal boundaries. Bénard attributed the striking patterns to flow due to buoyant forces acting in the bulk of the fluid. Rayleigh [2] later confirmed, through linear stability analysis, that buoyant forces do in fact generate convective cells. His findings, however, do not strictly apply to the configurations investigated by Bénard.

Bénard's incorrect conclusion was not categorically dismissed for at least another 50 years, at which time it was shown experimentally by Block [3] in 1956, and theoretically by Pearson [4] in 1958 that changes in surface tension, due to minor variations in the temperature of the fluid surface, were actually causing the observed convective cells. This convection mechanism is usually named Marangoni convection in recognition of his previous work [5]. Since that time, the linear stability of such configurations has been well analysed, especially in the case of a layer of infinite horizontal extent, that is, with an aspect ratio approaching infinity. These works have led to a deeper understanding of the fundamental physics at work in the problem. In this sense, experiments necessarily take place in finite vessels where the sidewalls can play an important role in the convective structure. Actually, it can be decisive in small boxes. For instance, experiments performed in small-aspect-ratio cylindrical vessels may show various very different patterns [6, 7].

The practical applications of BM convection are many and varied, and help to explain the sustained interest in the topic since Bénard's work. For example, in the realm of chemical engineering applications, Dijkstra [8] mentioned two applications [9, 10] in which mass transfer across an interface is strongly influenced by surface-tension effects.

Due to both the complexity of the theory involved in BM convection and the wide variety of experiments based on it, in this work we carry out only an introductory explanation of it which, nevertheless, permits a useful understanding of the main concepts involved in BM convection such as, for example, Bénard cells, aspect ratio, Rayleigh and Marangoni numbers, Crispation number and critical conditions. Because the experimental assembly is very simple and relatively cheap, the experiments carried out are very suggestive and the results obtained are clear and unambiguous, we recommend this device for use as a laboratory experiment for undergraduate students of nonlinear and fluid physics.

2. An intuitive understanding of Bénard–Marangoni convection

Convection in fluids has been a fruitful system for the study of nonlinear, nonequilibrium patterns for more than 100 years. The kind of convective transport we discuss here is called natural or free convection meaning that the flow is a response to forces acting within the body of the fluid [11, 12]. The force is most often gravity. One of the earliest descriptions of natural convection was written in the 1790s by Benjamin Thompson, but it was not until about 1900 that systematic experimental work was done by Henri Bénard. On the other hand, the preeminent theorist of convection in the early 20th century was John William Strutt, Lord Rayleigh. He attempted to explain Bénard's results in an article on convection published in 1916. It is now known that Rayleigh's theory does not apply to the system examined by Bénard who used shallow layers of whale oil, heated from below and open to the air above. Nevertheless, Rayleigh's work is the starting point for almost all modern theories on convection. Rayleigh's theory can be explained in the context of a model experiment in which a thin layer of fluid is confined between two flat, rigid, horizontal plates and completely fills the space between them, so that there is no free surface. In these experimental conditions, an imbalance of forces is needed to initiate a convective flow when the thin layer of fluid is heated from below, generating a gradient in temperature and density. If a parcel of warm fluid from near the bottom of the layer is displaced upwards slightly, it enters a region of greater average density and is therefore subject to an upward buoyant force. Similarly, if a parcel of cool fluid from near the top of the layer is displaced downwards, it becomes heavier than its surroundings and tends to sink. The buoyancy force is opposed by viscous drag and by heat diffusion. The drag force is always directed opposite to the motion of the fluid, and its magnitude is determined in part by an intrinsic property of the fluid, the kinematic viscosity.

On the other hand, the heat diffusion tends to equalize the temperature of a displaced parcel and its environment. The effect of heat diffusion can be explained by considering again a parcel of warm fluid displaced upwards from its equilibrium position into a cooler environment. According to the fundamental definition of heat, the molecules in the warm parcel must have a higher average speed than those in the surrounding cooler fluid. Molecules can freely cross the boundary that defines the parcel, and the effect of many such exchanges in both directions will be to equalize the average speeds of the two populations. The time required for a fluid parcel to reach thermal equilibrium with its surroundings depends in part on a property of the fluid, the thermal diffusivity.

Rayleigh's analysis shows that the mere existence of a temperature gradient is not enough to ensure the onset of convective flow. It is necessary for the buoyancy resulting from this gradient to exceed the dissipative effects of viscous drag and heat diffusion. The relation of these effects can be expressed as a dimensionless ratio: the buoyant force divided by the product of the viscous drag and the rate of heat diffusion. This ratio is called the *Rayleigh number*, R, which takes the following form,

$$R = \frac{g\alpha \Delta T d^3}{\nu \kappa} \tag{1}$$

where g denotes acceleration due to gravity, α is the coefficient of thermal volume expansion, ΔT is the vertical temperature gradient, ν is the kinematic viscosity, κ is the thermal diffusivity of the fluid and d is the thickness of the liquid layer. In the Rayleigh theory, convection begins when the Rayleigh number exceeds a critical value, R_c.

We must take into account that although the Rayleigh theory is remarkably successful in predicting the conditions necessary for the onset of convection in real fluids, even the more advanced theories on convection cannot account for all the observed features of fully developed convective circulation. If the evolution of flow cannot be deduced mathematically, however, at least a qualitative description is possible. In a fluid layer heated uniformly from below, the temperature gradient should be independent of the horizontal position and so it should be the resulting buoyant force. When the critical Rayleigh number is exceeded and the motionless equilibrium becomes unstable, the warm fluid therefore tends to rise everywhere and the cool fluid tends to sink everywhere. Both things obviously cannot happen at once: at any point the fluid can be ascending or descending, but it cannot move in both directions at the same place and time. This impasse is avoided by the spontaneous division of the layer into a pattern of convection polygonal cells, in each of which the fluid circulates in a closed orbit. Initially the polygons are somewhat irregular, having from four to seven sides, although the mean number is six. When the pattern is fully developed, it becomes an almost perfect array of regular hexagons, arranged as in a honeycomb (figure 1(a)). The centre of each hexagonal cell is a region of upwelling warm fluid, which spreads out over the upper surface and sinks at the perimeter, where adjacent cells are joined. The distance between central points of neighbour hexagonal cells defines the wavelength λ of the system (figure 1(b)). The tessellation of the fluid surface is one of the most attractive features of the convective phenomena, which becomes visible when marker particles, such as, for example, aluminium or graphite, are added to the fluid. From the linear stability theory [13], it is possible to determine at the onset of the convection the critical value of the Rayleigh number, R_c, whose value depends on the boundary conditions of the fluid layer. The critical Rayleigh number is the minimum of the stability limit, and occurs for a unique wavelength, λ_c. For a layer with a free upper surface (where the stress is zero) and a rigid bottom wall, the critical wavelength at the onset of instability is

$$\lambda_c \cong 2.342d \tag{2}$$

and the corresponding value of the Rayleigh number is $R_c \cong 1100.7$.

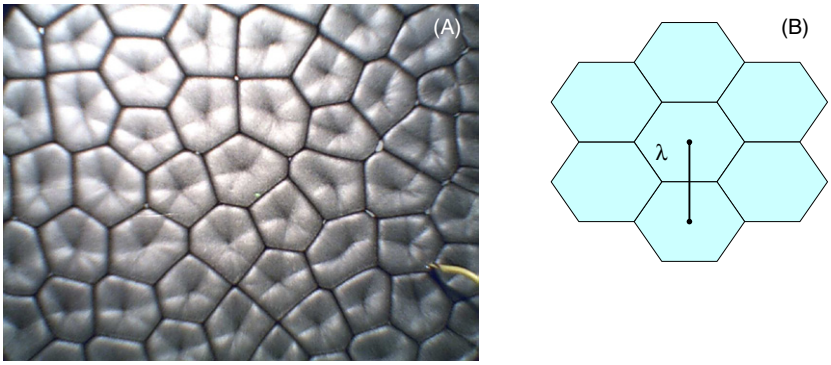

Figure 1. (a) Honeycomb-like cell pattern observed in Bénard convection open to air and (b) hexagon geometry showing the wavelength λ.

The main difference between the model experiment of Rayleigh and the Bénard experiment is the use or nonuse of two rigid boundaries to confine the liquid layer. In Bénard convection the upper surface of the liquid is open to the air and, in consequence, the flow is affected by the surface tension; indeed, surface tension is now recognized as the dominant influence in Bénard convection, being more important than the buoyant force. Surface tension is the cohesive force whose net effect is to minimize the surface area of a fluid. It can act as the propulsive force in a convective flow because the tension varies with temperature: like density, the surface tension is reduced as the temperature increases. Therefore any temperature gradient established across the surface of the liquid will be accompanied by a gradient in surface tension. The cooler regions will exhibit stronger surface tension and in the warmer regions the tension will be reduced. If the surface-tension gradient leads to an imbalance of forces, a flow will result. This effect was taken into account by a successful alternative theory introduced in 1958 by J R A Pearson [4]. When the surface tension is included in the convection analysis it is useful to use a new dimensionless ratio: the surface-tension gradient force divided by the product of the viscous drag and the rate of heat diffusion. This ratio is called the *Marangoni number*, M, which takes the form,

$$M = \frac{\gamma \Delta T d}{\rho \nu \kappa} \tag{3}$$

where γ denotes the temperature derivative of the surface tension and ρ is the density at a reference temperature (usually 20° C). In the context of this theory, as in the Rayleigh one, convection begins when the Marangoni number exceeds a critical value, M_c.

Convection driven by surface-tension gradients alters the contour of the surface, and its roughness increases with the layer thickness [14]. Regions of enhanced surface tension tend to pucker, so that they reduce their total exposed area. Thus, over the centre of each cell, the surface is depressed. A number of different studies have considered a more general case in which both density and surface-tension mechanisms act simultaneously, a situation usually termed as Bénard–Marangoni convection, which is the subject of the present work. The first study of BM convection in a planar horizontal fluid layer with a non-deformable free surface was performed by Nield [15], who showed that for steady convection the two destabilizing mechanisms reinforce one another. Nield obtained the following relationship between the Rayleigh number and the Marangoni number,

$$\frac{R}{R_{0c}} + \frac{M}{M_{0c}} \cong 1 + \varepsilon \tag{4}$$

where $R_{0c} = 680$ is the critical value of the Rayleigh number when there is no surface-tension gradient ($\gamma = 0$), and $M_{0c} = 81$ is the critical value of the Marangoni number in weightlessness ($g = 0$). ε is a dimensionless parameter that can take different values. For a given experiment, ε characterizes the distance to the threshold of the instability. In order to estimate the range of values for ε, Sarma [16] introduced the *Crispation number*, Cr,

$$Cr = \frac{\rho \nu \kappa}{\sigma d} \tag{5}$$

where σ is the surface tension. This author showed that if $Cr < 10^{-4}$ then ε takes a value near to 0, which means that surface deformations are probably negligible [17, 18].

Next, some interesting expressions can be obtained by combining the previous equations. For example, the following relationship can be obtained between the vertical temperature gradient and the thickness of the fluid layer by substituting equations (1) and (3) into (4) (and by taking $\varepsilon = 0$),

$$\Delta T(d) = \frac{\mu \kappa 680 \cdot 81}{81 \rho \alpha g d^3 + 680 \gamma d} \tag{6}$$

and $\mu = \rho \nu$.

On the other hand, an interesting relationship between the Rayleigh number and the Marangoni number can easily be obtained by dividing equation (1) by equation (3),

$$\frac{R}{M} = \left(\frac{\rho \alpha g}{\gamma} \right) d^2. \tag{7}$$

Equation (7) shows that the relative importance of the two effects involved in BM convection depends on the thickness of the liquid layer. In a typical convection experiment, the parameters between brackets (which depend on the liquid used) take constant values. In this way, the convection is controlled by surface-tension forces for small thickness of the liquid layer (that is, for high values of Marangoni number). On the other hand, the relative importance of the density gradient in convection increases with the increment of the thickness of the liquid layer (high values of Rayleigh number).

3. Experimental setup

The experimental device used in this work which can be used as a laboratory experiment for undergraduate students is very simple and is composed of the following components:

(i) special oil container,
(ii) heater,
(iii) two thermocouples,
(iv) rheostat,
(v) two multimeters,
(vi) CCD camera,
(vii) silicone oil (Rhodorsil 47V 500),
(viii) aluminium particles used as a tracer (Panreac, reference 141098).

Figure 2(a) shows the experimental setup consisting of a special cylindrical vessel with an inner diameter D filled with a silicone oil and heated from below with a free air upper surface. The free surface of the liquid is horizontal and in contact with the atmosphere, without a lid. The oil container, designed specifically for this experiment, has its bottom and wall manufactured from aluminium and teflon, respectively. In this respect, aluminium was selected as a good conductor and teflon as a good insulator. Figure 2(b) shows the dimensions of this important component.

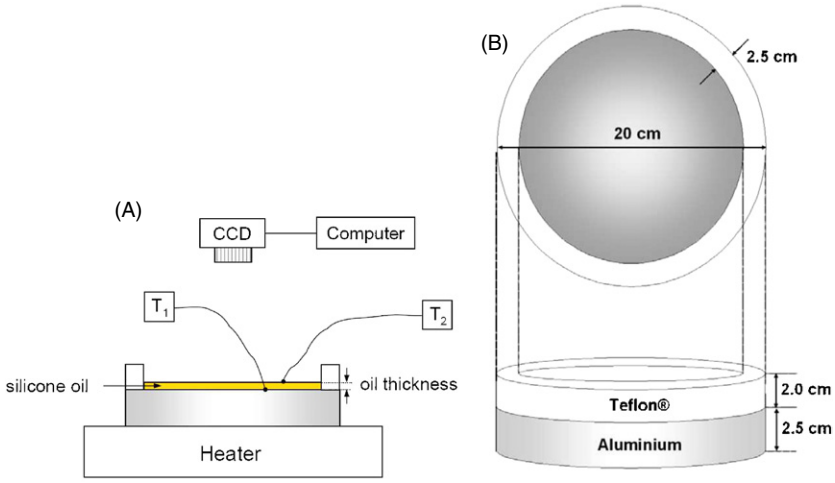

Figure 2. (a) Experimental setup and (b) geometry and dimensions of the oil container for the Rayleigh–Bénard experiment.

Table 1. Physical properties of the silicone oil Rhodorsil 47V 500.

Symbol	Name	Value
ρ	Density at 20 °C	9.57×10^{2} kg m^{-3}
α	Coefficient of thermal volume expansion	7.67×10^{-4} K^{-1}
ν	Kinematic viscosity	7.40×10^{-5} m^{2} s^{-1}
κ	Thermal diffusivity	1.14×10^{-7} m^{2} s^{-1}
σ	Surface tension	2.50×10^{-2} kg m^{-3}
γ	Temperature derivative of the surface tension	2.67×10^{-5} N m^{-1} K^{-1}

A CCD camera (see figure 2(a)) located at the top of the oil container and connected to a computer allows the experiment to be filmed for further image processing. In a typical experiment, the oil container has a calculated amount of silicone oil with a determined thickness. Silicone oil has been previously used [19] as model fluid to observe convection cells (commonly known as Bénard cells). The main physical characteristics of this commercial silicone oil are shown in table 1.

Two thermocouples are placed carefully (see figure 2(a)) on the bottom of the container (T1) and on the oil surface (T2). The size of the temperature probe must be small. In our case, the temperature probes used have spherical shape with a diameter of 1 mm. Aluminium particles were added to make the convective flow visible.

The temperature gradient in the oil layer is increased by controlling the power supplied to the heater. Figure 3 shows the simple electrical circuit that permits us to control carefully the heat supplied to the oil. The heater is connected to a rheostat and the power supplied is measured with two multimeters which act as a voltmeter and ammeter, respectively.

In order to obtain good results and reproducibility in the experiments the location of the experimental assembly in the laboratory is very important. As is usual in heat transmission experiments, air flows should be prevented, and the temperature of the room should be kept as constant as possible.

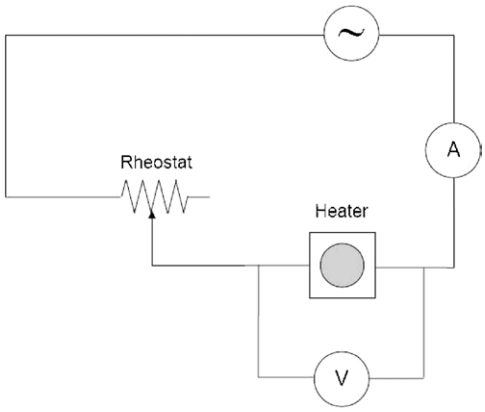

Figure 3. Electrical circuit used for the analysis of the onset of Bénard–Marangoni convection in a horizontal layer of fluid.

Although in this work we are interested in convection patterns in cylinders of large aspect ratio $\Gamma = D/d$, the setup allows us to make experiments in containers of small to medium aspect ratio, $5 \leqslant \Gamma \leqslant 10$, by placing crystal cylinders inside the oil. New effects due to confinement are expected, such as, for example, the dependence of the critical magnitudes on the aspect ratio [7].

During the experiment, the transition between a conductive to a convective regime can be observed. Bénard cells obtained experimentally with the setup described above are shown in figure 1(a). In each of these cells, fluid particles in the middle of the cells rise. The rising fluid loses heat by thermal conduction at the free top wall, travels horizontally, and then sinks at the boundaries of the cell. For a steady cellular pattern, the continuous generation of kinetic energy is balanced by viscous dissipation. The generation of kinetic energy is maintained by continuous release of potential energy due to heating at the bottom and cooling at the top.

4. Results and discussion

Once convection starts, a cellular pattern arises whose cells approximate a hexagonal geometry after stationary conditions are achieved (figure 1(a)). The presence of defects in the oil container, non-homogeneous heating from below, or even the presence of air flow at the free surface can lead to defect formation and then to irregular hexagonal cells. Figure 4 shows the mean wavelength of the cellular pattern for four different depths. The mean wavelength is calculated as the mean value of the distance between the middle points of all consecutive cells in the medium (see figure 1(b) for a reference). The solid line corresponds to the theoretical value $\lambda_c(d)$ predicted by the linear stability theory (2) at the onset of convection. As the fluid depth is increased, the uncertainty of the wavelength also increases due to either the presence of more defects in the liquid, or to the fact that the pattern did not attain a stationary condition[4]. The presence of a supercritical flow where $R > R_c$ could be the cause of the differences between the theoretical line and the experimental data, since linear theory predicts a continuum of wavelengths that are greater and less than λ_c, and there is no preferred wavelength to the flow [11, 13].

[4] Since this work is oriented to an undergraduate laboratory, we think it important to note the possible sources of error in determining the most significant parameters at the criticality.

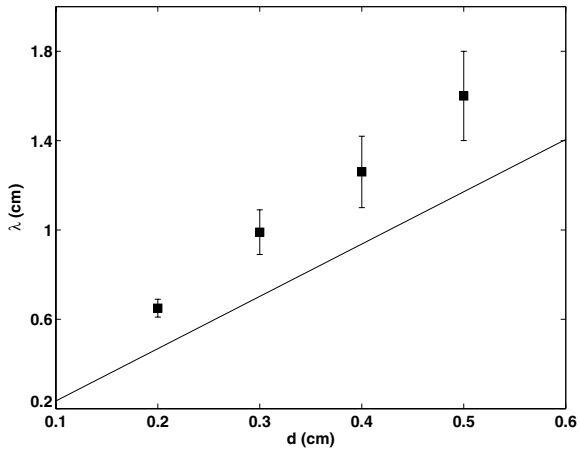

Figure 4. Wavelength as a function of the thickness of the liquid layer d once convection is fully developed. The solid line corresponds to the theoretical value predicted by the linear stability theory (2) at the onset of convection.

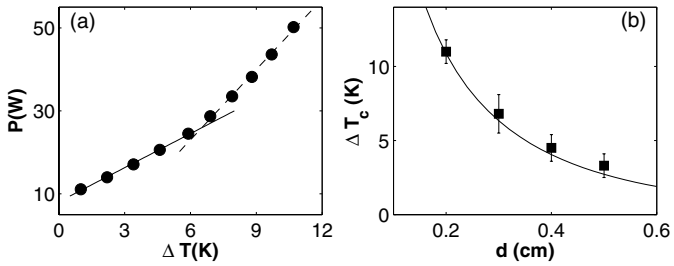

Figure 5. (a) Heating power $P = I\Delta V$ as a function of the vertical gradient of temperature ΔT for $d = 3$ mm. Lines correspond to a linear fit of the experimental data. (b) Theoretical curve, equation (6), of the critical value of the temperature gradient as a function of the thickness of the liquid layer. Dots correspond to experimental data.

In general, to obtain the critical Rayleigh number is a difficult task, since as the Rayleigh number of the flow tends to R_c, the settling time for the flow (i.e. the time taken for the flow to reach a steady state) tends to infinity. Therefore, the Schmidt–Milverton principle [20] is used for the detection of the onset of thermal instability and the determination of both the critical Rayleigh and Marangoni numbers for different liquid layer thickness. This principle is so direct and simple that it has served as the basis for all later experiments in this subject [13]. It establishes that one of the main differences between the conduction and convection mechanism of heat transfer is the efficiency of heat dissipation. In fact, convection is a more efficient dissipative mechanism than conduction. As a consequence, when a thin liquid layer is heated from below by applying a heating power through an electrical resistance, it exhibits different behaviour. In practice, figure 5(a) shows two different linear intervals when the heating power, P, which can be numerically expressed as $P = I\Delta V$ (Joule effect), is plotted versus the vertical temperature gradient. The same figure shows the lines that fit the experimental data. The slope of the convection interval is higher than the slope of the previous conduction interval due to the effective thermal conductivity increasing beyond its conduction value. The cross point of the two lines can be understood as the critical temperature gradient for which the change of heat transfer mechanism (from conduction to convection) takes place.

Table 2. Rayleigh and Marangoni critical numbers obtained experimentally as a function of the liquid layer thickness d.

d (mm)	R_c	M_c
2	78.4	72.86
3	163.6	67.52
4	256.6	59.58
5	367.5	54.62

The critical value of the temperature gradient for each liquid layer thickness is then calculated as the cross point of the two lines described above for every thickness of the liquid layer. Figure 5(b) shows experimental and theoretical results for the critical value of the temperature gradient versus the thickness of the liquid layer. The theoretical curve has been obtained using equation (6). Previously, we evaluated the Crispation number (Cr) in order to test the validity of this equation. By using the data from table 1 we obtained values of the Crispation number in the range 6.4×10^{-5} to 1.62×10^{-4} ($d = 2$ mm) for layer thicknesses of 5 mm and 2 mm, respectively. For these conditions, ε tends to zero, and equation (6) can be used. The results obtained evidence a decrease in the critical temperature gradient with increment of thickness of the liquid layer.

The excellent agreement between the theoretical data and the experimental data shown in figure 5(b) seems to prove the validity of the Nield equation (4). The overlapping of the error bars is due to the simplicity of the experimental assembly used which is affected by several errors, such as for example, the uncertainty in the exact position of the temperature bore, which has a thickness of 1 mm. Nevertheless, in our particular opinion, the interest of the experiments shown in this work does not diminish for this reason.

Finally, by using the critical values of the temperature gradient, the critical values of the Rayleigh and Marangoni numbers, equations (1)–(3), are evaluated for different values of the thickness of the liquid layer d (see table 2). These results show an increase of the critical value of the Rayleigh number and a decrease of the critical Marangoni number with increment of layer thickness, respectively, as expected from linear stability theory. This behaviour shows that the relative importance of the two effects involved in BM convection, buoyancy forces and surface tension, depend on the thickness of the liquid layer. The ratio $r = (R_c/R_{c0})/(M_c/M_{c0})$ (or also using equation (7)) gives an idea of the relative importance of the buoyancy and surface-tension effects. Here, this ratio varies from 0.13 to 0.80, so surface-tension effects are predominant, although buoyancy forces become gradually important when the thickness of the liquid layer is increased.

5. Conclusions

In spite of the theoretical complexity of BM convection, in this work we carry out an introductory analysis that allows a qualitative understanding of the main concepts involved such as, for example, Bénard cells, aspect ratio, Rayleigh and Marangoni numbers, Crispation number and critical conditions. On the other hand, the observation of Bénard cells and some of their qualitative properties seems to justify an approach to this topic which has been little studied from a didactic point of view. As the experimental assembly shown in this work is very simple and the results obtained are clear and unambiguous, we recommend this setup for use as a laboratory experiment for undergraduate students of nonlinear and fluid physics.

Acknowledgments

The authors acknowledge financial support from Consejería de Innovación, Ciencia y Empresa de la Junta de Andalucía and Ministerio de Educación y Ciencia (Spain) under research grant FIS2004-03006.

References

[1] Bénard H 1900 Les tourbillons cellulaires dans une nappe liquide *Rev. Gén. Sci. Pure Appl.* **11** 1261–71
[2] Rayleigh (Lord) 1916 On convective currents in a horizontal layer of fluid when the higher temperature is on the under side *Phil. Mag.* **32** 529–46
[3] Block M J 1956 Surface tension as the cause of Bénard cells and surface deformation in a liquid *Nature* **178** 650–1
[4] Pearson J R A 1958 On convection cells induced by surface tension *J. Fluid Mech.* **4** 489–500
[5] Marangoni C G M 1871 Ueber die Ausbreitung der Tropfen einer Flüssigkeit auf der Oberfläche einer anderen *Ann. Phys. Chem. (Poggendorf)* **143** 337–54
[6] Koschmieder E L and Prahl S A 1990 Surface-tension-driven Bénard convection in small containers *J. Fluid Mech.* **215** 571–83
[7] Pasquetti R, Cerisier P and Le Niliot C 1994 Laboratory and numerical investigations on cylindrical Bénard–Marangoni convection *Phys. Fluids* **14** 277–88
[8] Dijkstra H A 1992 On the structure of cellular solutions in Rayleigh–Bénard–Marangoni flows in small-aspect-ratio containers *J. Fluid Mech.* **243** 73–102
[9] Patberg W B, Koers A, Steenge W D E and Drinkenburg A A H 1983 Effectiveness of mass-transfer in a packed distillation column in relation to surface-tension gradients *Chem. Eng. Sci.* **38** 917–23
[10] Zuiderweg F J and Harmens A 1958 The influence of surface phenomena on the performance of distillation columns *Chem. Eng. Sci.* **9** 89–90
[11] Normand C, Pomeau Y and Velarde M G 1977 Convective instability: physicists approach *Rev. Mod. Phys.* **49** 581–624
[12] Velarde M G and Normand C 1980 Convection *Sci. Am.* **243** 92–3
[13] Chandrasekhar S 1981 *Hydrodynamic and Hydromagnetic Stability* (New York: Dover)
[14] Cerisier P, Jamond J, Pantaloni J and Charmet J C 1984 Déformation de la surface libre en convection de Bénard–Marangoni *J. Physique* **45** 405–11
[15] Nield D A 1964 Surface tension and buoyancy effects in cellular convection *J. Fluid Mech.* **19** 341–52
[16] Sarma G S R 1982 *4th Int. Conf. on Physico-Chemical Hydrodynamics (New York)*
[17] Pantaloni J, Bailleux R, Salan J and Velarde M G 1979 Rayleigh–Bénard–Marangoni instability: new experimental results *J. Non-Equilib. Thermod.* **4** 201–18
[18] Tokaruk W A, Molteno T C A and Morris S W 2000 Bénard–Marangoni convection in two layered liquids *Phys. Rev. Lett.* **84** 3590–3
[19] Hashim I and Wilson S K 1999 The onset of Bénard–Marangoni convection in a horizontal layer of fluid *Int. J. Eng. Sci.* **37** 643–62
[20] Schmidt R J and Milverton S W 1935 On the instability of a fluid when heated from below *Proc. R. Soc.* **152** 586–94